Proceedings of ITC18, 2008

Spectroscopic diagnostics for spatial density distribution of plasmoid by pellet injection in Large Helical Device

G. Motojima, R. Sakamoto, M. Goto, H. Yamada and LHD experimental group

National Institute for Fusion Science,322-6 Oroshi-cho, Toki 509-5292, Japan

In order to investigate the behavior of the plasmoid which is the pellet ablatant ionized by background plasma, two-dimensional imaging measurements of high-speed spectroscopy using a fast camera has been developed in the Large Helical Device. The diagnostic system provides the density distribution of the plasmoid. The density distribution is determined by the Stark broadening width of Balmer-β line. The Stark broadening profile can be evaluated from the intensity ratio measured with narrow-band optical filters having different full width at half maximum. The two-dimensional images of the plasmoid by the fast camera connected to a bifurcated fiber scope with two objective lenses are obtained. As an initial result from the imaging measurements, it is shown that the plasmoid density is in the order of 10^{23} m^{-3}.

Keywords: pellet injection, plasmoid, helical device, two-dimensional imaging measurements, spectroscopy

1 Introduction

Solid hydrogen pellet injection is a primary technique for efficient core plasma fueling in fusion devices. The pellet injection is sure to play a important role in next-step devices such as ITER and also will be one of promising candidates for particle refueling in a future fusion reactor. In particular, the importance of the pellet injection is increased in the high central density operation required for a helical reactor [1].

When pellets are injected into a hot, magnetically confined plasma, pellet particles are ablated by heat flux from a background plasma. The pellet is immediately surrounded by its neutral cloud which is generated by the ablation of the pellet. The neutral cloud has a effect of shielding from the ambient background plasma. Subsequently the neutral cloud is ionized and expanded in the direction parallel to the magnetic field lines. Here, the ionized pellet material is referred to as a plasmoid.

The pellet ablation and subsequent behavior of the plasmoid are key elements to determine the characteristics of pellet fueling. Extensive experiments have been devoted to the clarification of fueling characteristics of the pellet [2]. In particular, recent studies have been focused on the drift of the plasmoid [3]. The drift of the plasmoid may be attributed to an $\boldsymbol{E} \times \boldsymbol{B}$ drift that arises from a vertical polarization in the ablation cloud due to the magnetic field gradient [4]. The behavior of the plasmoid following ablating process has a primary effect on the pellet mass deposition. Therefore, the understanding of not only the pellet ablation but also subsequent behavior of the plasmoid allows the optimization of the pellet fueling. As for the pellet ablation, the identification of the position in the pellet ablation is of great importance. In LHD, three-dimensional observation system with stereoscopic analysis using a fast camera has been developed [5]. The position of the pellet ablation can be precisely identified by using this method. Concerning the behavior of the plasmoid, the quantitative evaluation of the pellet particles transferred by the plasmoid provides the understanding of the homogenization process of the plasmoid. The process of the homogenization has been demonstrated in numerical calculations. Moreover, the density and temperature of the plasmoid has been measured by spectroscopic diagnostics [6, 7]. However, quantitative two-dimensional evaluation of the plasmoid parameters has not yet been achieved. The objective of this study is to evaluate the two-dimensional density distribution in the plasmoid quantitatively by imaging measurements with high-speed spectroscopic diagnostics.

The rest of the paper is organized as follows. The principle of the high-speed spectroscopic analysis is described in Section 2. In Section 3, the experimental setup is presented. The initial experimental results are shown in Section 4. Summary is given in Section 5.

2 Imaging measurements of High-speed spectroscopy

The spectrum of Balmer-line depends on the density and temperature of the plasmoid. Here, the emission from the background plasma can be ignored, since the density of the plasmoid is about several hundred times larger than that of the background plasma, resulting that the emission from the plasma is much smaller than that from the plasmoid. The electron density can be determined from the Stark broadening profile of the Balmer-α or Balmer-β line. Figure 1 shows examples of spectra in the range of wavelength from 400 to 800 nm for (a) low density (n_e = 1.0×10^{22} m^{-3}) and (b) high density (n_e = 9.0×10^{23} m^{-3}). The same electron temperature is assumed at 1.0 eV for both cases (the value is based on the results from ref. [7]). Here, the spectra are estimated from the fitting with the the-

author's e-mail: gen@lhd.nifs.ac.jp

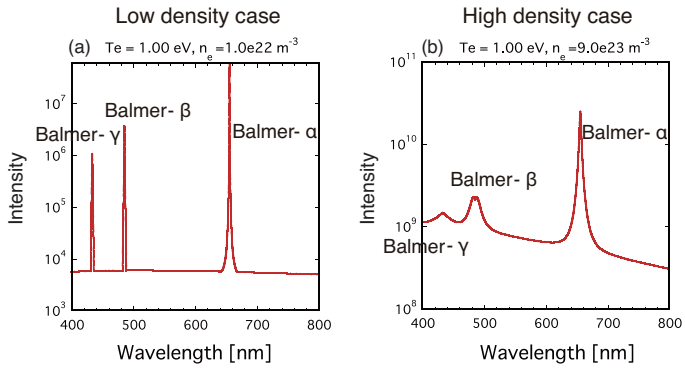

Fig. 1 Spectra in the range of wavelength from 400-800 nm for (a) low density ($n_e = 1.0\times10^{22}$ m^{-3}) and (b) high density ($n_e = 9.0\times10^{23}$ m^{-3}). The same electron temperature is selected. Intensity is expressed in logarithmic scale.

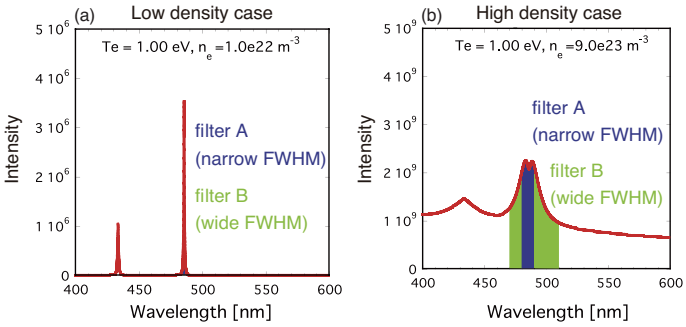

Fig. 2 Spectra of the Balmer-β and Balmer-γ lines with a constant background for (a) low density ($n_e = 1.0\times10^{22}$ m^{-3}) and (b) high density ($n_e = 9.0\times10^{23}$ m^{-3}). Intensity is expressed in linear scale.

oretical data based on the collision-radietive model [8, 9]. Only the Balmer-α, β, and γ lines appear as discrete lines and other series lines appear as a continuum spectrum. In low density case, the line profile is peaked. While, in high density case, the line profile is broader. It is found that the line profile depends on the electron density. The characteristics make possible the evaluation of the electron density.

The Stark broadening width can be estimated from the intensity ratio measured with narrow-band optical filters having different full width at half maximum (FWHM). Figure 2 shows the extended figure of Fig. 1 around Balmer-β line. In low density case, there is almost no difference in the intensity between wide and narrow FWHMs due to the peaked line profile. While, in high density case, the intensity difference becomes large due to the broader line profile, resulting that the ratio of intensity measured with narrow FWHM to that measured with wide FWHM becomes small.

In this study, we concentrate on the Balmer-β line (center wavelength : 486.1 nm) to evaluate the density of plasmoid. The filter parameters suitable for various presumed densities (10^{22} – 10^{24} m^{-3}) and temperatures (0.9-1.2 eV) in a plasmoid were selected using the spectra es-

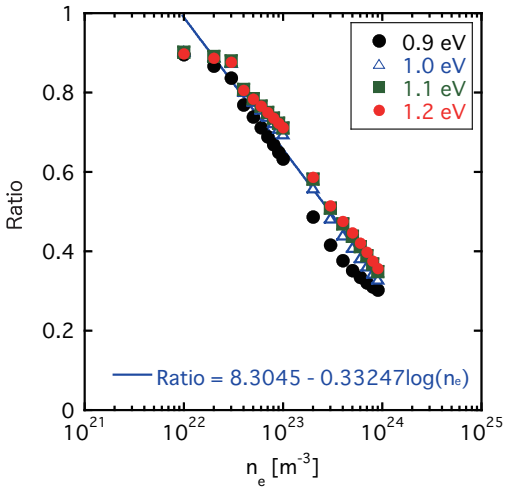

Fig. 3 Dependence of the logarithm of density on the ratio of the intensity measured with FWHM of 5 nm to that measured with wide FWHM of 20 nm. Solid line shows logarithm fitting of the data. The fitting line is used in analysis.

timated from theoretical data. The ranges of density and temperature are assumed by the results from spectrometer measurement of plasmoid in LHD [7]. Figure 3 shows the dependence of the logarithm of electron density on the ratio of the intensity measured with FWHM of 5 nm to that measured with wide FWHM of 20 nm. The ratio is approximately proportional to the logarithm of plasmoid density. The ratio is small with increasing electron density. With this filter combination, dependence of the plasmoid temperature can be ignored, and we are able to measure the plasmoid density in the range from 10^{22} to 10^{24} m^{-3}.

3 Experimental Setup

In this section, the spectroscopic diagnostics system for density distribution of plasmoid is explained. Figure 4(a) shows a horizontally elongated poloidal cross section of the LHD and in-situ pipe gun type 10 barrel pellet injector. The plasmoid can be observed just behind the pipe gun pellet injector and parallel to the injection axis :namely, the line of sight is consistent with the pellet injection axis. The emission from the plasmoid is evenly divided by a half mirror, as shown in Fig. 4(b).

A bifurcated fiber scope with two objective lenses is used in this spectroscopic system [5]. The scope is composed of a pair of 50000 element quarts fiber scopes with a stainless-steel flexible protective tube. The overall length is 15 m and the bifurcated portions are about 5 m in length. Each objective lens, which has a field of view of 15 degree, with different filters selected in Sec. 2 is used. Two images which are viewed from the same line of sight just behind the pellet injector are obtained.

The images are focused onto a single fast camera (Vision Research Inc., Phantom V7) so that the simultaneity

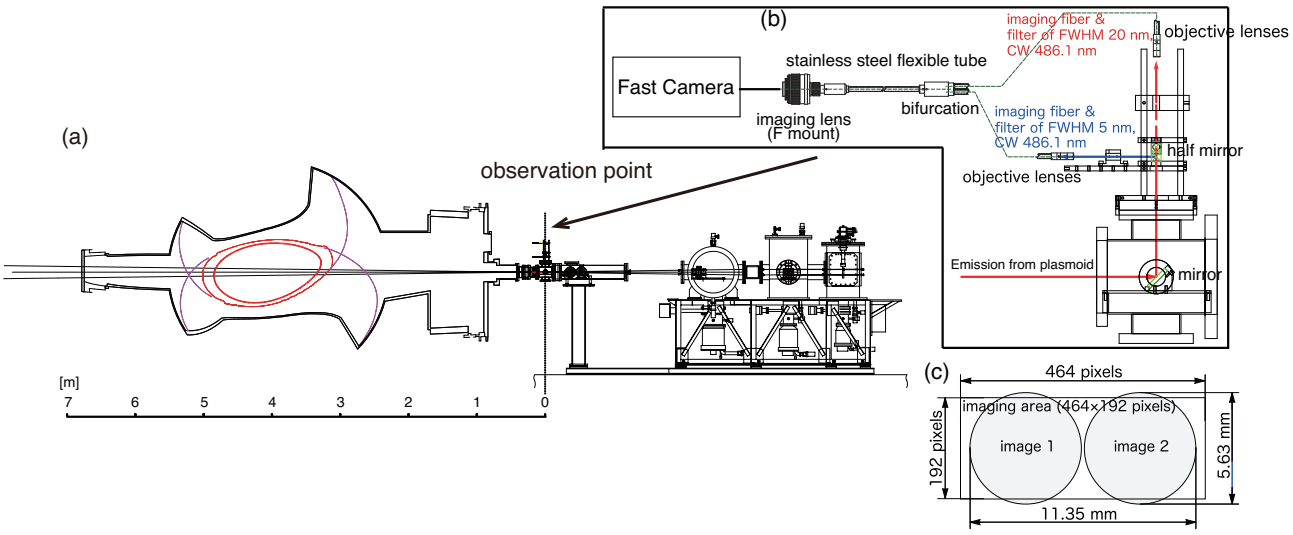

Fig. 4 (a) Cross-sectional drawing of the LHD vacuum vessel and fuelling pellet injector, which is equipped with 10 barrels independent barrels (b) enlarged view of observation point where the imaging measurements are equipped (c) imaging area on the sensor of the fast camera.

is ensured. The fast camera is equipped with a 12 bit self-resetting complementary metal oxide semiconductor sensor (SR-CMOS). The frame rate and the exposure time are selected to be 2000 fps with a resolution of 464 × 192 pixels and 2 μs, respectively. The bundled end is connected to an imaging lens which can project a pair of images onto the imaging sensor, as shown in Fig. 4(c).

4 Results

The initial results of two-dimensional imaging measurements by high-speed spectroscopy were obtained. Figure 5 shows typical images of the plasmoid with the filters having (a) FWHM 5 nm and (b) FWHM 20 nm. The pellet is injected to the NBI plasma with central electron temperature of 1.5 keV. Here, the identity of the two fields of view is confirmed by the strong correlation between two images. The intensity of the image with the filter of FWHM 20 nm is stronger than that of image with the filter of FWHM 5 nm. The plasmoid seems to be expanded to the direction parallel to the magnetic field line. The emission intensity distribution of two images in the direction perpendicular to the magnetic field line passing through the maximum intensity point is shown in Fig. 6(a). The difference of intensity is observed in the pellet ablatant. Since it is difficult to evaluate the ratio of intensity in the outer region of the plasmoid due to small intensity and/or lower density than that of assumption, the analysis is limited to the region around the plasmoid. Figure 6(b) shows the ratio of intensity between two images in the direction perpendicular to the magnetic field line passing through the maximum intensity point. In the center of plasmoid which has strong intensity, the ratio is close to 1 that means the density in the order of 10^{22} m^{-3}. On the other hand, in the region around the center of plasmoid, minimum of the ratio is about 0.6 that means the density in the order of 10^{23} m^{-3}. Figure 7(a)

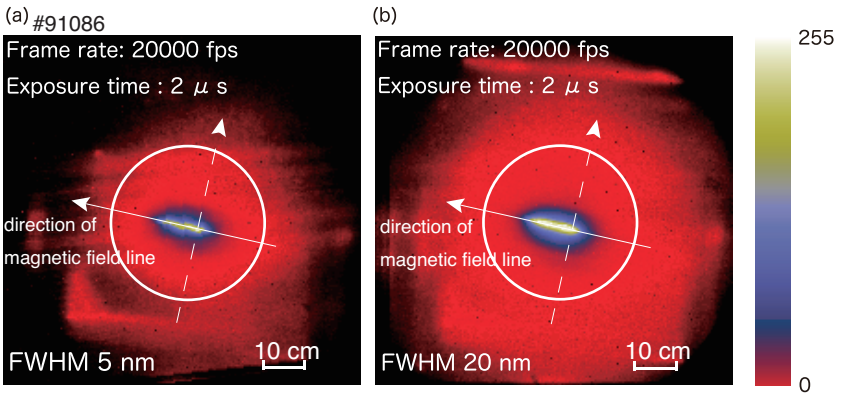

Fig. 5 Typical images of plasmoid with the filters having (a) FWHM of 5 nm and (b) FWHM of 20 nm. Analysis is made within the circular line. Solid line shows the direction of the magnetic field line and dot line shows the direction perpendicular to the magnetic field line.

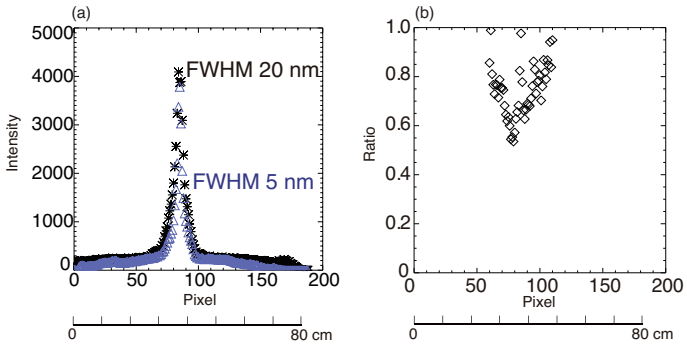

Fig. 6 (a) Emission intensity distribution and (b) ratio of two images in the direction perpendicular to the magnetic field line passing through the maximum intensity point. Asterisk symbol shows the intensity with FWHM of 20 nm and triangle symbol shows the intensity with FWHM of 5 nm.

shows the density distribution in the plasmoid. Here, gray zone shows the region having large error because of small intensity. The density of the plasmoid is over 10^{22} m^{-3} and the plasmoid measures 20 cm wide. The plasmoid density is in the order of 10^{23} m^{-3} except for the center region of the pellet ablatant. In the center region of the plasmoid, the density seems to be lower. The reason may be attributed to the unexpected temperature range. However, further studies are necessary. Figure 7 (b) shows the electron density distribution in the direction perpendicular to the magnetic field line passing through the maximum intensity point. The maximum electron density at 2.3×10^{23} m^{-3} is observed.

5 Summary

In order to obtain the two-dimensional plasmoid density distribution quantitatively, imaging measurements of high-speed spectroscopic system using a fast camera has been developed. The density of the plasmoid is evaluated by the width of the Stark broadening in Balmer-β line. The Stark broadening can be estimated by comparing the difference in emission intensity from the plasmoid between narrow-band optical filters having different FWHM. The most suitable a pair of filters which have the same central wavelength of 486.1 nm and different FWHM of 5 nm and 20 nm was selected by the spectra estimated from the fitting with the theoretical data. As an initial result, the density distribution of the plasmoid by imaging measurements was obtained. Here we show that the plasmoid density is in the order of 10^{23} m^{-3}. In future, the three-Dimensional distribution of the density in the plasmoid will be evaluated by using tomography under the assumption that the structure of the plasmoid is rotational axial-symmetry around the magnetic field line.

Acknowledgements

The authors are grateful to the LHD operation group. This study was supported by NIFS08ULPP521.

[1] O. Mitarai *et al.*, Proc. 22nd IAEA Fusion Energy Conference, Geneva, FT/P3-19 (2008); also available at http://www-pub.iaea.org/MTCD/Meetings/FEC2008/ft_p3-19.pdf
[2] B. Pégourié, Plasma Phys. Control. Fusion **49**, R87 (2007).
[3] P. T. Lang *et al.*, Phys. Rev. Lett. **79**, 1487 (1997).
[4] V. Rozhansky *et al.*, Plasma Phys. Control. Fusion **37**, 399 (1995).
[5] R. Sakamoto *et al.*, Rev. Scient. Inst. **76**, 103502 (2005).
[6] D. H. McNeill *et al.*, Phys. Fluids B **3**, 1994 (1991).
[7] M. Goto *et al.*, Plasma Phys. Control. Fusion **49**, 1163 (2007).
[8] C. Stehle and R. Hutcheon, Astron. Astrophys. Suppl. Ser. **140**, 93 (1999).
[9] T. Fujimoto, Plasma Spectroscopy (Oxford: Oxford University Press) (2004).

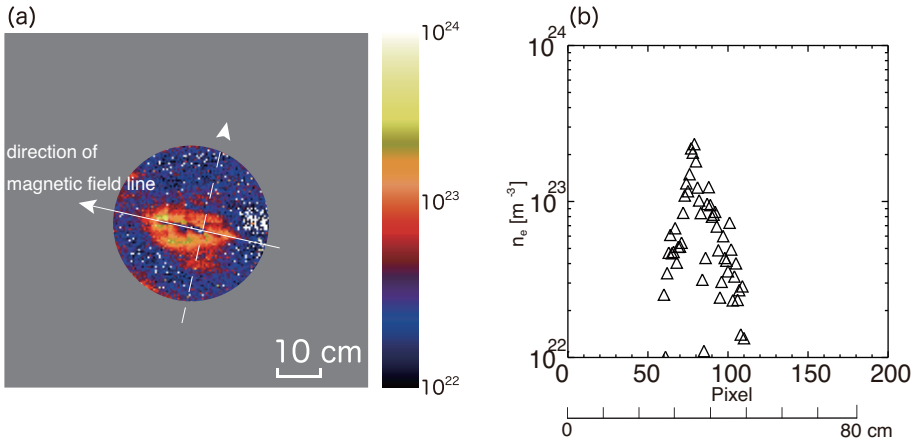

Fig. 7 (a) Density distribution in plasmoid and (b) electron density distribution along the dot line in the direction perpendicular to the magnetic field line passing through the maximum intensity point. Here, dot line shows the direction of the magnetic field line and dot line shows the direction perpendicular to the magnetic field line.